Supplementary Material for "Heterogeneity Induces Cyclops states in Kuramoto Networks with Higher-Mode Coupling"

Maxim I. Bolotov[1], Lev A. Smirnov[1], Vyacheslav O. Munyayev[1], Grigory V. Osipov[1], and Igor Belykh[2]
[1]*Department of Control Theory, Lobachevsky State University of Nizhny Novgorod, 23 Gagarin Avenue, Nizhny Novgorod, 603022, Russia*
[2]*Department of Mathematics and Statistics and Neuroscience Institute, Georgia State University, P.O. Box 4110, Atlanta, Georgia, 30302-410, USA*

I. DETAILED DERIVATION OF THE COLLECTIVE COORDINATE REDUCTION

This section provides the full derivation of the reduced mesoscopic model introduced in the main text. Our goal is to identify stationary cyclops and two-cluster states in the full heterogeneous oscillator network described by Eq. (1) of the main paper and construct their approximate representations using a collective coordinate reduction.

The stationary state of system Eq. (1) for nonidentical oscillators can be conveniently analyzed in a rotating reference frame. We define the relative phases as $\varphi_n = \theta_n - \Omega t$, where Ω is the common rotational frequency of the system and $n = 1, \ldots, N$. We fix the phase of the Nth (solitary) oscillator as the reference point, choosing $\varphi_N = 0$.

To simplify notation, we introduce the phase difference relative to the solitary oscillator:

$$\varphi_n = \theta_n - \theta_N, \quad n = 1, 2, \ldots, N-1. \tag{S.1}$$

This substitution effectively eliminates the absolute phase of the solitary node, anchoring the system and reducing the analysis to relative phase dynamics.

Substituting (S.1) into Eq. (1) in the main text and subtracting the equation for the Nth oscillator from each of the others yields the following system for $n = 1, 2, \ldots, N-1$:

$$m\ddot{\varphi}_n + \dot{\varphi}_n = \omega_n - \omega_N + \sum_{q=1}^{2} \frac{\varepsilon_q}{N} \left[\sum_{k=1}^{N-1} \left(\sin\left(q(\varphi_k - \varphi_n) - \alpha_q\right) - \sin\left(q\varphi_k - \alpha_q\right) \right) - \sin(q\varphi_n + \alpha_q) + \sin\alpha_q \right]. \tag{S.2}$$

To express the system in terms of intrinsic frequency mismatches, we introduce the detuning parameters:

$$\Delta_n = \omega_n - \omega_N, \tag{S.3}$$

which quantify the deviation of each oscillator's natural frequency from that of the solitary node.

To facilitate further analysis, it is convenient to rewrite the system in complex form. Using the identity $\sin(\phi) = \mathrm{Im}\left[e^{i\phi}\right]$, we transform Eq. (S.2) into the following equivalent representation:

$$m\ddot{\varphi}_n + \dot{\varphi}_n = \Delta_n + \sum_{q=1}^{2} \mathrm{Im}\left[\frac{\varepsilon_q e^{-i\alpha_q}}{N} \left(\sum_{k=1}^{N-1} e^{iq\varphi_k} + 1 \right) \left(e^{-iq\varphi_n} - 1 \right) \right], \tag{S.4}$$

where $n = 1, 2, \ldots, N-1$.

For compactness, we introduce the vector notation

$$\boldsymbol{\varphi} = (\varphi_1, \varphi_2, \ldots, \varphi_{N-1}), \tag{S.5}$$

and define the nonlinear right-hand side as

$$\Phi_n(\boldsymbol{\varphi}, \Delta_n) = \Delta_n + \sum_{q=1}^{2} \mathrm{Im}\left[\frac{\varepsilon_q e^{-i\alpha_q}}{N} \left(\sum_{k=1}^{N-1} e^{iq\varphi_k} + 1 \right) \left(e^{-iq\varphi_n} - 1 \right) \right]. \tag{S.6}$$

This allows the system to be expressed compactly as

$$m\ddot{\varphi}_n + \dot{\varphi}_n = \Phi_n(\boldsymbol{\varphi}, \Delta_n), \tag{S.7}$$

which we will use as the starting point for the reduction via collective coordinates.

The stationary solutions of Eq. (S.7) correspond to uniformly rotating states of the original system (1). These solutions are defined by the set

$$\boldsymbol{\varphi}^* = (\varphi_1^*, \varphi_2^*, \ldots, \varphi_{N-1}^*), \tag{S.8}$$

which satisfy the nonlinear algebraic system

$$\Phi_n(\boldsymbol{\varphi}^*, \Delta_n) = 0, \quad n = 1, 2, \ldots, N-1. \tag{S.9}$$

To analyze the linear stability of the stationary solution (S.8), we introduce small perturbations $\delta\varphi_n(t)$ and linearize Eq. (S.7) around $\boldsymbol{\varphi}^*$, which yields the variational equation:

$$m\delta\ddot{\varphi}_n + \delta\dot{\varphi}_n = \sum_{k=1}^{N-1} \left.\frac{\partial \Phi_n}{\partial \varphi_k}\right|_{\boldsymbol{\varphi}^*} \delta\varphi_k, \quad n = 1, 2, \ldots, N-1. \tag{S.10}$$

Assuming solutions of the form $\delta\varphi_n(t) = D_n e^{\lambda t}$, the linearized system reduces to the eigenvalue problem

$$\boldsymbol{M_P}\,\mathbf{D} = \Lambda\,\mathbf{D}, \tag{S.11}$$

where $\mathbf{D} = (D_1, D_2, \ldots, D_{N-1})^T$, $\Lambda = m\lambda^2 + \lambda$, and $\boldsymbol{M_P} = \left.\frac{\partial \boldsymbol{\Phi}}{\partial \boldsymbol{\varphi}}\right|_{\boldsymbol{\varphi}^*}$ is the Jacobian matrix evaluated at the stationary solution.

The eigenvalues Λ_k ($k = 1, \ldots, N-1$) obtained from Eq. (S.11) yield the corresponding set of dynamical eigenvalues λ_k ($k = 1, \ldots, 2N-2$), which determine the linear stability of the stationary state (S.8). Directly identifying such stationary states to be used in the linear stability analysis in large heterogeneous oscillator networks is computationally demanding and often elusive.

To overcome this obstacle, we introduce a reduction approach based on the collective coordinate framework [1–6]. This method approximates the phase dynamics of clustered states using a low-dimensional ansatz that captures the essential structure of cyclops and two-cluster configurations. As we demonstrate below, this reduction not only enables efficient computation of candidate solutions but also yields reliable predictions for the stability.

We now apply the collective coordinate method to approximate the dynamics of cyclops states. This approach is based on constructing a liner ansatz $\hat{\boldsymbol{\varphi}}$ for the oscillator phases,

$$\varphi_n(t) \approx \hat{\varphi}_n(\boldsymbol{\Gamma}(t); \Delta_n), \quad n = 1, 2, \ldots, 2K, \tag{S.12}$$

where $\boldsymbol{\Gamma}(t)$ is a vector of collective coordinates that evolve in time and parameterize the effective dynamics of the cyclops state. Given that the natural frequencies ω_n (and thus the detunings Δ_n) are uniformly distributed, the relative phases $\varphi_n(t)$ within each cluster can be well-approximated by linear functions of the form:

$$\begin{aligned} \varphi_n(t) &\approx \hat{\varphi}_n(t) = \psi_1(t) + \chi_1(t)\Delta_n, \quad n = 1, \ldots, K, \\ \varphi_n(t) &\approx \hat{\varphi}_n(t) = \psi_2(t) + \chi_2(t)\Delta_n, \quad n = K+1, \ldots, 2K, \end{aligned} \tag{S.13}$$

where $\psi_\mu(t)$ represents the collective phase of the μth cluster and $\chi_\mu(t)$ characterizes the linear phase distortion within the cluster due to frequency heterogeneity. The product $\chi_\mu(t)\Delta_n$ thus captures the deviation of the nth oscillator's phase from its cluster average $\psi_\mu(t)$, with $\mu = 1, 2$ denoting the cluster index.

In this representation, the dynamics of the full phase difference system (S.7) are approximated by the evolution of four collective coordinates:

$$\boldsymbol{\Gamma}(t) = \left(\psi_1(t), \psi_2(t), \chi_1(t), \chi_2(t)\right), \tag{S.14}$$

which together define a mesoscopic description of the cyclops regime.

To derive the reduced equations, we substitute the ansatz (S.13) into the full system (S.4), which introduces an approximation error. The residual (or error) for each oscillator is given by

$$\xi_n = m\ddot{\hat{\varphi}}_n + \dot{\hat{\varphi}}_n - \Delta_n - \sum_{q=1}^{Q} \mathrm{Im}\left[\frac{\varepsilon_q e^{-i\alpha_q}}{N}\left(\sum_{k=1}^{N-1} e^{iq\hat{\varphi}_k} + 1\right)\left(e^{-iq\hat{\varphi}_n} - 1\right)\right], \tag{S.15}$$

and the full error vector is

$$\boldsymbol{\xi} = (\xi_1, \xi_2, \ldots, \xi_{2K}). \tag{S.16}$$

Following the standard collective coordinate approach [6], we minimize the error by requiring that it is orthogonal to the tangent space of the ansatz manifold. This yields the following orthogonality conditions:

$$\langle \boldsymbol{\xi}, \frac{\partial \hat{\boldsymbol{\varphi}}}{\partial \psi_1} \rangle = 0, \quad \langle \boldsymbol{\xi}, \frac{\partial \hat{\boldsymbol{\varphi}}}{\partial \psi_2} \rangle = 0, \quad \langle \boldsymbol{\xi}, \frac{\partial \hat{\boldsymbol{\varphi}}}{\partial \chi_1} \rangle = 0, \quad \langle \boldsymbol{\xi}, \frac{\partial \hat{\boldsymbol{\varphi}}}{\partial \chi_2} \rangle = 0, \tag{S.17}$$

where $\langle \cdot, \cdot \rangle$ denotes the Euclidean scalar product.

The corresponding derivatives of the ansatz vector with respect to the collective coordinates are

$$\frac{\partial \hat{\boldsymbol{\varphi}}}{\partial \psi_1} = \left(\underbrace{1 \ \dots \ 1}_{K} \ \underbrace{0 \ \dots \ 0}_{K} \right)^T, \quad \frac{\partial \hat{\boldsymbol{\varphi}}}{\partial \psi_2} = \left(\underbrace{0 \ \dots \ 0}_{K} \ \underbrace{1 \ \dots \ 1}_{K} \right)^T. \tag{S.18}$$

Substituting into Eq. (S.17) and evaluating the inner products, we obtain the following coupled equations for the cluster-averaged phases $\psi_\mu(t)$ and phase distortions $\chi_\mu(t)$:

$$\begin{aligned} m\ddot{\psi}_\mu + \dot{\psi}_\mu + (m\ddot{\chi}_\mu + \dot{\chi}_\mu - 1) \frac{1}{K} \sum_{k=(\mu-1)K+1}^{\mu K} \Delta_k \\ = \sum_{q=1}^{Q} \mathrm{Im} \Bigg[\frac{\varepsilon_q e^{-i\alpha_q}}{N} \Big(1 + \sum_{k=1}^{K} e^{iq(\psi_1 + \chi_1 \Delta_k)} + \sum_{k=K+1}^{2K} e^{iq(\psi_2 + \chi_2 \Delta_k)} \Big) \\ \times \left(\frac{1}{K} \sum_{k=(\mu-1)K+1}^{\mu K} e^{-iq(\psi_\mu + \chi_\mu \Delta_k)} - 1 \right) \Bigg], \end{aligned} \tag{S.19}$$

where $\mu = 1, 2$ indexes the two clusters. For convenience, we introduce the following notation:

$$\delta_\mu = \frac{1}{K} \sum_{k=(\mu-1)K+1}^{\mu K} \Delta_k, \quad S_\mu^{(q)} = \frac{1}{K} \sum_{k=(\mu-1)K+1}^{\mu K} e^{iq\chi_\mu \Delta_k}, \tag{S.20}$$

where δ_μ is the average frequency detuning within the μth cluster, and $S_\mu^{(q)}$ is the qth-order Kuramoto-type order parameter describing the internal phase distribution in that cluster. Substituting these expressions into Eq. (S.19) yields a more compact form for the projected equation onto $\partial \hat{\boldsymbol{\varphi}} / \partial \psi_\mu$:

$$\begin{aligned} m\ddot{\psi}_\mu + \dot{\psi}_\mu + \delta_\mu (m\ddot{\chi}_\mu + \dot{\chi}_\mu - 1) = \sum_{q=1}^{Q} \mathrm{Im} \Bigg[\frac{\varepsilon_q e^{-i\alpha_q}}{N} \Big(1 + K S_1^{(q)} e^{iq\psi_1} + K S_2^{(q)} e^{iq\psi_2} \Big) \\ \times \Big(S_\mu^{(q)*} e^{-iq\psi_\mu} - 1 \Big) \Bigg]. \end{aligned} \tag{S.21}$$

To complete the Galerkin projection, we now consider the derivatives of the ansatz with respect to χ_1 and χ_2:

$$\frac{\partial \hat{\boldsymbol{\varphi}}}{\partial \chi_1} = \left(\Delta_1 \ \dots \ \Delta_K \ \underbrace{0 \ \dots \ 0}_{K} \right)^T, \quad \frac{\partial \hat{\boldsymbol{\varphi}}}{\partial \chi_2} = \left(\underbrace{0 \ \dots \ 0}_{K} \ \Delta_{K+1} \ \dots \ \Delta_{2K} \right)^T. \tag{S.22}$$

We further introduce

$$\sigma_\mu^2 = \frac{1}{K} \sum_{k=(\mu-1)K+1}^{\mu K} \Delta_k^2, \quad J_\mu^{(q)} = \frac{1}{K} \sum_{k=(\mu-1)K+1}^{\mu K} \Delta_k e^{iq\chi_\mu \Delta_k}, \tag{S.23}$$

where σ_μ^2 is the second moment of th frequency distribution in the μth cluster, and $J_\mu^{(q)}$ is a weighted qth-order order parameter incorporating the detuning. Projecting onto $\partial \hat{\boldsymbol{\varphi}} / \partial \chi_\mu$, we obtain the second pair of equations:

$$\begin{aligned} \delta_\mu (m\ddot{\psi}_\mu + \dot{\psi}_\mu) + \sigma_\mu^2 (m\ddot{\chi}_\mu + \dot{\chi}_\mu - 1) = \sum_{q=1}^{Q} \mathrm{Im} \Bigg[\frac{\varepsilon_q e^{-i\alpha_q}}{N} \Big(1 + K S_1^{(q)} e^{iq\psi_1} + K S_2^{(q)} e^{iq\psi_2} \Big) \\ \times \Big(J_\mu^{(q)*} e^{-iq\psi_\mu} - \delta_\mu \Big) \Bigg]. \end{aligned} \tag{S.24}$$

Solving Eqs. (S.21) and (S.24) simultaneously gives the evolution of the collective coordinates $\psi_\mu(t)$ and $\chi_\mu(t)$. For practical implementation, we rewrite them in a decoupled form as:

$$m\ddot{\psi}_\mu + \dot{\psi}_\mu = \sum_{q=1}^{Q} \mathrm{Im}\left[\frac{\varepsilon_q e^{-i\alpha_q}}{N}\left(1 + KS_1^{(q)}e^{iq\psi_1} + KS_2^{(q)}e^{iq\psi_2}\right)\left(\frac{\sigma_\mu^2 S_\mu^{(q)*} - \delta_\mu J_\mu^{(q)*}}{\sigma_\mu^2 - \delta_\mu^2}e^{-iq\psi_\mu} - 1\right)\right], \tag{S.25}$$

$$m\ddot{\chi}_\mu + \dot{\chi}_\mu = 1 + \frac{1}{\sigma_\mu^2 + \delta_\mu^2}\sum_{q=1}^{Q} \mathrm{Im}\left[\frac{\varepsilon_q e^{-i\alpha_q}}{N}\left(1 + KS_1^{(q)}e^{iq\psi_1} + KS_2^{(q)}e^{iq\psi_2}\right)\left(J_\mu^{(q)*} - \delta_\mu S_\mu^{(q)*}\right)e^{-iq\psi_\mu}\right]. \tag{S.26}$$

Equations (S.25) and (S.26) define the reduced eight-dimensional system (4) in the main text, governing the collective dynamics of clustered oscillators in the presence of frequency heterogeneity. Thus, the stationary solutions

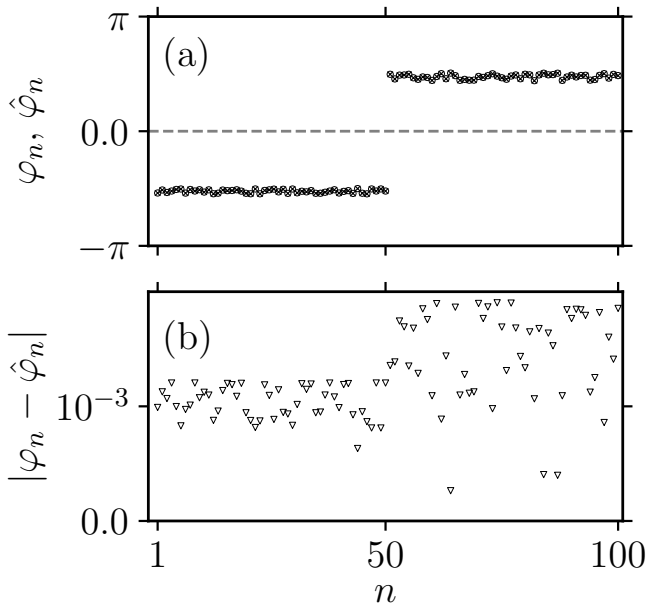

Supplementary Figure 1: Comparison of stationary phases in the full and reduced systems. (a) Phase values from the full system (S.7) (crosses) and the reduced collective coordinate approximation (S.30) (circles) based on the solution of Eqs. (S.25), (S.26). (b) Absolute error $|\varphi_n - \hat{\varphi}_n|$ between the exact and approximated phases, which remains below 2×10^{-3} for all oscillators. Parameters: $N = 101$, $\alpha_1 = 1.57$, $\varepsilon_1 = 1.0$, $\varepsilon_2 = 0.03$, $\alpha_2 = 0.1$, $\nu = 0.005$.

$$\mathbf{\Gamma}^* = (\psi_1^*, \psi_2^*, \chi_1^*, \chi_2^*) \tag{S.27}$$

satisfying the nonlinear system

$$\begin{aligned} &F_\mu(\psi_1, \psi_2, \chi_1, \chi_2) = 0, \\ &G_\mu(\psi_1, \psi_2, \chi_1, \chi_2) = 0, \quad \mu = 1, 2 \end{aligned} \tag{S.28}$$

define stationary cyclops or two-cluster modes of the reduced system (S.25), (S.26).

These solutions can be used to reconstruct approximate stationary phase configurations of the full difference system (S.7). Specifically, the collective coordinates $\mathbf{\Gamma}^*$ yield the approximate phase differences

$$\hat{\varphi}_n^* = \psi_1^* + \chi_1^*\Delta_n, \quad n = 1, \ldots, K, \tag{S.29}$$

$$\hat{\varphi}_n^* = \psi_2^* + \chi_2^*\Delta_n, \quad n = K+1, \ldots, 2K, \tag{S.30}$$

which follow directly from the ansatz (S.13).

Supplementary Figure 1 confirms the accuracy of the reduced model by comparing its predicted stationary phase profile with the full system. The collective coordinate approximation derived from Eqs. (S.25), (S.26) closely matches

the stationary solution of the full phase difference system (S.7) for a cyclops state with $N = 101$, $\alpha_1 = 1.57$, $\varepsilon_1 = 1.0$, $\varepsilon_2 = 0.03$, $\alpha_2 = 0.1$, and $\nu = 0.005$. As shown in Supplementary Fig. 1b, the maximum deviation between the approximated and full phase values does not exceed 2×10^{-3}.

To assess the linear stability of the stationary solution (S.27), we consider small perturbations $\delta\psi_\mu(t)$ and $\delta\chi_\mu(t)$ around each collective coordinate and linearize the reduced system (S.25)-(S.26) in its vicinity. This yields the linearized equations

$$m\delta\ddot{\psi}_\mu + \delta\dot{\psi}_\mu = \sum_{k=1}^{2} \left[\left.\frac{\partial F_\mu}{\partial \psi_k}\right|_{\mathbf{\Gamma^*}} \delta\psi_k + \left.\frac{\partial F_\mu}{\partial \chi_k}\right|_{\mathbf{\Gamma^*}} \delta\chi_k \right], \tag{S.31}$$

$$m\delta\ddot{\chi}_\mu + \delta\dot{\chi}_\mu = \sum_{k=1}^{2} \left[\left.\frac{\partial G_\mu}{\partial \psi_k}\right|_{\mathbf{\Gamma^*}} \delta\psi_k + \left.\frac{\partial G_\mu}{\partial \chi_k}\right|_{\mathbf{\Gamma^*}} \delta\chi_k \right], \quad \mu = 1, 2, \tag{S.32}$$

where all partial derivatives are evaluated at the stationary point $\mathbf{\Gamma^*}$. Substituting exponential perturbations $\delta\psi_\mu = B_\mu e^{\lambda t}$ and $\delta\chi_\mu = C_\mu e^{\lambda t}$ reduces the problem to a standard eigenvalue problem:

$$\boldsymbol{M_C}(B_1, B_2, C_1, C_2)^T = \Lambda(B_1, B_2, C_1, C_2)^T, \tag{S.33}$$

where the Jacobian matrix $\boldsymbol{M_C}$ is defined as

$$\boldsymbol{M_C} = \left(\begin{array}{cccc} \frac{\partial F_1}{\partial \psi_1} & \frac{\partial F_1}{\partial \psi_2} & \frac{\partial F_1}{\partial \chi_1} & \frac{\partial F_1}{\partial \chi_2} \\ \frac{\partial F_2}{\partial \psi_1} & \frac{\partial F_2}{\partial \psi_2} & \frac{\partial F_2}{\partial \chi_1} & \frac{\partial F_2}{\partial \chi_2} \\ \frac{\partial G_1}{\partial \psi_1} & \frac{\partial G_1}{\partial \psi_2} & \frac{\partial G_1}{\partial \chi_1} & \frac{\partial G_1}{\partial \chi_2} \\ \frac{\partial G_2}{\partial \psi_1} & \frac{\partial G_2}{\partial \psi_2} & \frac{\partial G_2}{\partial \chi_1} & \frac{\partial G_2}{\partial \chi_2} \end{array} \right)\Bigg|_{\mathbf{\Gamma^*}}. \tag{S.34}$$

The eigenvalues $\Lambda_k = m\lambda_k^2 + \lambda_k$ $(k = 1, 2, 3, 4)$ of matrix $\boldsymbol{M_C}$ provide a set of eigenvalues λ_k $(k = 1, 2, \ldots, 8)$ of the stationary mode (S.27), which determine its stability.

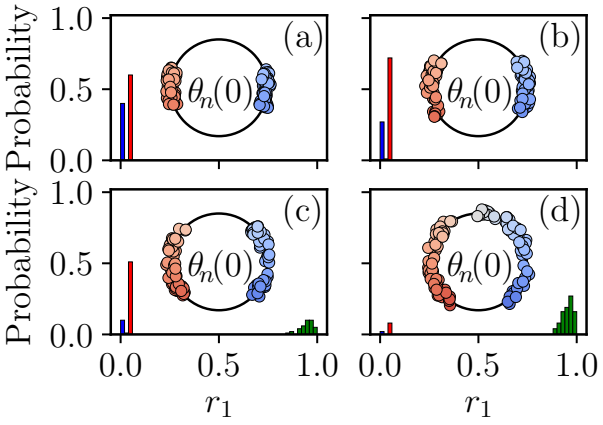

Supplementary Figure 2: Probabilistic emergence of cyclops and two-cluster states in the Kuramoto network (1). Probabilities are computed from 100 trials with initial phases $\theta_n(0)$ drawn from two clusters centered at fixed offsets, with half-widths $\delta = 0.4$ (a), $\delta = 0.6$ (b), $\delta = 0.8$ (c), and $\delta = 1.0$ (d). Initial velocities $\dot{\theta}_n(0)$ are uniformly distributed in $[-0.5, 0.5]$. Blue: cyclops states; red: two-cluster states; green: near-synchronous regimes with $r_1 \approx 1$. Cyclops states appear with probabilities up to 0.4, indicating spontaneous formation of a solitary oscillator from symmetric initial conditions. Parameters correspond to the red circle in Fig. 1a.

II. ATTRACTION PROBABILITIES OF CYCLOPS AND TWO-CLUSTER STATES IN THE KURAMOTO MODEL

Supplementary Figure 2 illustrates that both cyclops and two-cluster states induced by frequency heterogeneity can arise with appreciable probability when the system is initialized from broad two-cluster phase distributions. In

particular, two-cluster states dominate with probabilities up to 70% across a range of initial spreads. Cyclops states also emerge with probabilities reaching 40%, even though the solitary oscillator is not explicitly present in the initial conditions. This indicates that the solitary node can self-organize from symmetric configurations. While the prevalence of cyclops and two-cluster states decreases for wider initial spreads, these results highlight that heterogeneity promotes the spontaneous formation of such regimes over a sizable portion of phase space.

III. BEYOND PHASE MODELS: HETEROGENEITY-INDUCED STABILIZATION OF CYCLOPS STATES IN NETWORKS OF STUART–LANDAU OSCILLATORS

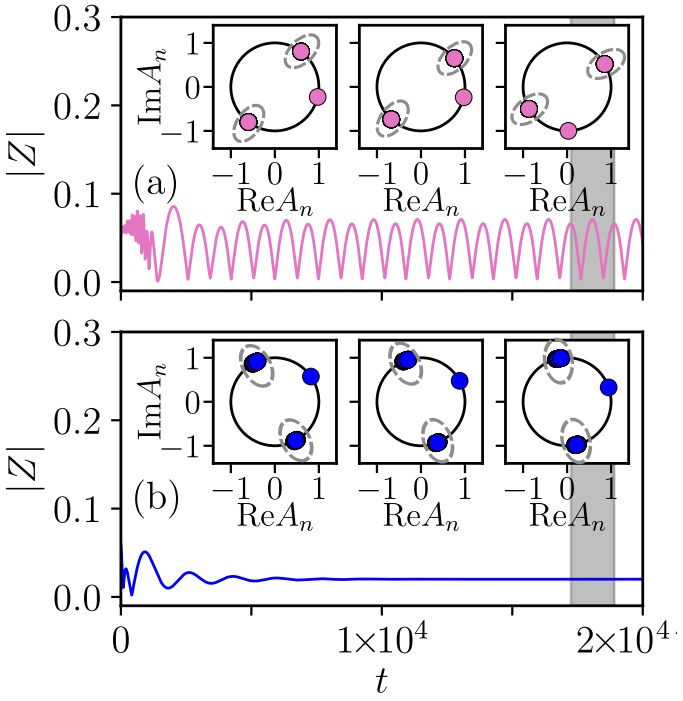

Supplementary Figure 3: Stabilization of the cyclops state in a network of Stuart–Landau oscillators (S.35). (a, b) Dynamics of the order parameter amplitude $|Z(t)|$ together with its transient evolution. Insets: snapshots of the oscillator states A_n taken at different times within the gray-highlighted interval of $|Z(t)|$, with clusters outlined by a grey dotted line. (a) Breather cyclops state ($\mathcal{P} = 0.99$, $\nu = 0.0$). (b) Stabilized stationary cyclops state ($\mathcal{P} = 0.66$, $\nu = 3 \times 10^{-5}$); two-cluster states occur in the remaining runs ($\mathcal{P} = 0.34$, not shown). Probabilities $\mathcal{P}$ quantify the fraction of runs converging to each state, computed over 100 trials with uniformly distributed initial conditions in a small neighborhood of a single limit cycle. Parameters: $N = 101$, $\omega_0 = 0.0$, $\gamma = 10.0$, $\varepsilon_1 = 0.07$, $\varepsilon_2 = 0.003$, $\alpha_1 = 1.56$, $\alpha_2 = 0.1$.

We further investigate whether amplitude–phase dynamics can exhibit similar heterogeneity-induced stabilization. For this purpose, we analyze networks of Stuart–Landau oscillators with higher-harmonic coupling in the phase dynamics and weak amplitude variations. This class of models serves as a generic normal form for Andronov–Hopf bifurcations, capturing both amplitude and phase effects. Introducing frequency heterogeneity leads to the emergence of stable cyclops states. These results reinforce the generality of the mechanism and indicate that the stabilizing influence of disorder extends beyond purely phase-reduced descriptions to richer oscillator models. The presence of amplitude dynamics does not preclude the constructive role of heterogeneity in stabilizing multi-cluster states.

We consider a system of non-identical Stuart–Landau oscillators, described by the complex amplitudes A_n, which evolve according to

$$\dot{A}_n = \gamma(1 + i\omega_n)A_n - \gamma|A_n|^2 A_n + \frac{\varepsilon_1 e^{-i\alpha_1}}{N}\sum_{k=1}^{N} A_k + \frac{\varepsilon_2 e^{-i\alpha_2}}{N}\sum_{k=1}^{N} A_k^2 A_n^*, \tag{S.35}$$

where γ sets the time scale of the dynamics. The natural frequencies ω_n are drawn from a uniform distribution over the interval $[\omega_0 - \nu, \omega_0 + \nu]$, with mean frequency ω_0 and distribution half-width ν. The global coupling comprises

two distinct harmonics: a linear term with strength ε_1 and phase shift α_1, and a nonlinear term with strength ε_2 and phase shift α_2.

The degree of global synchrony is quantified by the complex order parameter

$$Z(t) = \frac{1}{N}\sum_{k=1}^{N} A_k(t), \tag{S.36}$$

whose modulus $|Z(t)|$ measures the oscillation amplitude coherence. We now demonstrate that frequency heterogeneity ($\nu > 0$) can stabilize the breathing dynamics of the cyclops state. For the parameter set $N = 101$, $\omega_0 = 0.0$, $\gamma = 10.0$, $\varepsilon_1 = 0.07$, $\varepsilon_2 = 0.003$, $\alpha_1 = 1.56$, $\alpha_2 = 0.1$, which supports a cyclops state, the system's behavior depends critically on ν. In the homogeneous case ($\nu = 0$), the system evolves into a breather cyclops state: clusters undergo persistent periodic oscillations relative to a solitary element, as seen in the dynamics of $|Z(t)|$ (Supplementary Fig. 3a). Notably, this regime appears from uniform phase distributions and amplitude spreads around 20% with probability close to one [not shown]. Introducing a small frequency heterogeneity ($\nu = 3 \times 10^{-5}$) suppresses these collective breather oscillations. This damping effect stabilizes a stationary cyclops state, characterized by a constant order parameter amplitude and fixed phase relationships between the clusters and the solitary element (Supplementary Fig. 3b). The heterogeneity-induced stationary cyclops inherits the structural properties of the breathing regime and remains the prevalent attractor under random initial conditions. As in the Winfree network (Fig. 4), two-cluster states also appear in the remaining runs ($\mathcal{P} = 0.34$, not shown).

[1] S. M. Cox and G. A. Gottwald, Physica D: Nonlinear Phenomena **216**, 307 (2006).
[2] G. A. Gottwald, Chaos: An Interdisciplinary Journal of Nonlinear Science **25** (2015).
[3] E. J. Hancock and G. A. Gottwald, Physical Review E **98**, 012307 (2018).
[4] L. D. Smith and G. A. Gottwald, Chaos: An Interdisciplinary Journal of Nonlinear Science **29** (2019).
[5] R. Berner, A. Lu, and I. M. Sokolov, Chaos: An Interdisciplinary Journal of Nonlinear Science **33**, 073138 (2023).
[6] L. D. Smith and G. A. Gottwald, Chaos: An Interdisciplinary Journal of Nonlinear Science **30** (2020).